Performance of a LiBr water absorption chiller operating with plate heat exchangers

M. de Vega [a,*], J.A. Almendros-Ibañez [a], G. Ruiz [b]

[a] *Departamento de Ingeniería Térmica y de Fluidos, Universidad Carlos III de Madrid, Avda. Universidad 30, 28911 Leganés, Madrid, Spain*

[b] *Now at: Unidad de Eficiencia Energética, Departamento de I + D, Besel S.A., Avda. Mediterráneo 22, 28912 Leganés, Madrid, Spain*

Abstract

This paper studies the performance of a lithium bromide water absorption chiller operating with plate heat exchangers (PHE). The overall heat transfer coefficients in the desorber, the condenser and the solution heat recoverer are calculated using the correlations provided in the literature for evaporation, condensation and liquid to liquid heat transfer in PHEs. The variable parameters are the external driving temperatures. In the desorber, the inlet temperature of the hot fluid ranges from 75 °C to 105 °C. In the condenser and the absorber, the inlet temperature of the cooling water goes from 20 °C to 40 °C. The coefficient of performance (COP) obtained ranges from 0.5 to 0.8 for cooling duties ranging from 2 kW to 12 kW. The chiller response to different hot fluid temperatures and circulated mass flow rates is also presented. The per formance and the internal parameters of the chiller at part load are, therefore, calculated. A higher efficiency results when the solution pumped from the absorber to the desorber decreases. The heat transfer analysis of the PHEs is also presented. The overall heat transfer coefficient in the desorber, equal to 790 W/m^2 K at the design conditions, is also analysed at part load. The condenser performance can be represented by a similar relationship found in conventional air cooled condensers.

Keywords: LiBr water absorption; Plate heat exchanger

1. Introduction

Absorption chillers using the LiBr water mixture have become one of the well accepted choices to overcome the environmental problems associated with the use of traditional refrigerants: CFCs and HCFCs. Consequently, large capacity direct fired and waste heat driven cooling systems have been studied and commercialised. Besides, it is difficult to extend their use to small sized air conditioning systems. This possibility seems to be promising since the temperature required in the heating source to power the desorber of the LiBr H_2O solution (less than 120 °C) may be provided by solar energy systems with low cost solar collectors

* Corresponding author. Tel.: +34 91 6249913; fax: +34 91 6249430.
E mail address: mdevega@ing.uc3m.es (M. de Vega).

Nomenclature

A	heat transfer area (m^2)
Bo	boiling number
COP	coefficient of performance
c_P	specific heat (kJ/kg K)
D_h	hydraulic diameter (m)
Eff	efficiency
h	specific enthalpy (kJ/kg)
m	mass flow rate (kg/h)
G	mass flux (kg/m^2 s)
Nu	Nusselt number
P	pressure (Pa)
Pr	Prandlt number
Q	heat transfer rate (kW)
R	fouling resistance (m^2 K/W)
Re	Reynolds number
t	temperature (°C)
U	global heat transfer coefficient (W/m^2 K)
w	specific work (kJ/kg)
x	solution concentration

Greek symbols

α	heat transfer coefficient (W/m^2 K)
η	pump efficiency
μ	viscosity of liquid phase (N/m s^2)
ρ	density (kg/m^3)
Δt	log mean temperature difference (°C)

Subscripts

in

[1 3]. One of the main constraints for the development of these small air conditioning units is the size required, which is still, by far, larger than the size of the conventional mechanical compression systems. To this effect, the use of compact heat exchangers in absorption systems needs to be investigated.

In order to increase the cooling capacity to volume ratio in absorption systems, we are working on a LiBr H_2O absorption chiller prototype employing plate heat exchangers in the desorber, the condenser and the solution heat recoverer. We are primarily interested in the analysis of the thermal and thermodynamic theoretical performance of this single effect chiller. The results are presented here.

Plate heat exchangers (PHE) are frequently employed in the food and chemical industry and are primarily used in liquid to liquid heat exchange duties. Thus, performance in single phase applications is extensively documented [4 6]. Recently, new theoretical and experimental efforts have been developed for the use of PHEs in evaporation and condensation processes [7 10]. Nevertheless, only a little information is available describing the operation of absorption chillers with PHEs [11,12].

Many works referring to ideal thermodynamic simulations of absorption cycles are available in the literature [13 16]. In most of these works, sensitivity analysis is done on the basis of the internal operating conditions: condensing temperature and final absorption and desorption temperatures. This is mainly due to the fact that the heat transfer equations are not considered in the simulations. Instead, we propose to predict the operational characteristics as a function of the external driving conditions: inlet temperatures of the cooling water and the hot fluid, respectively, entering the condenser and the desorber. In the present paper, in order to study the performance of the single effect LiBr H_2O absorption machine, the thermodynamic absorption cycle is coupled with the heat transfer characteristics of the selected plate heat exchangers. The results obtained will be used as a predictive tool for the performance of the system over a complete set of external conditions, as will correspond to a complete operation during a whole season. This whole season operation will provide a more realistic seasonal coefficient of performance that could be used to compare the performance of absorption chillers with PHEs with other types of machines. This will be, in the near future, verified with the results obtained in the experimental device, which is under construction.

2. Description of the system

The single effect absorption system consists of the following components: absorber, desorber, vapour separator, condenser, evaporator, heat recoverer, expansion and throttle valves and solution pump. The system is schematically shown in Fig. 1.

The distinguishing feature of the present system is that it incorporates plate heat exchangers: the desorber (fed by a liquid heat source); the condenser and the heat recoverer employed to preheat the solution on its way to the desorber. In the desorber, the external hot fluid (for example, pressurised hot water, heated by concentrators or vacuum tube solar collectors) provides the heat to boil the solution. Superheated refrigerant vapour, which separates from the solution, is generated. Traditionally, the desorber and the condenser are contained in the same vessel. According to the configuration of our experiment, two separate heat exchangers are

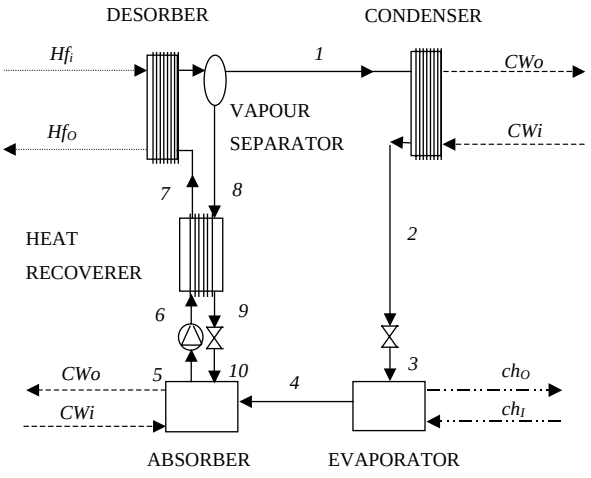

Fig. 1. Schematic diagram of the absorption chiller configuration.

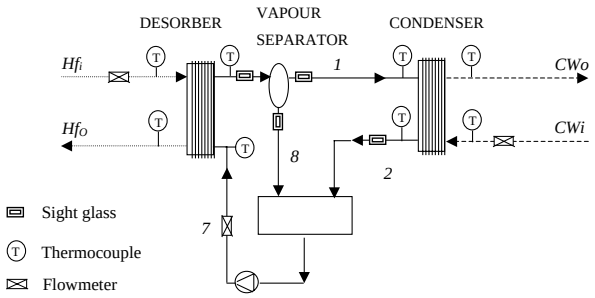

Fig. 2. Schematic diagram of the experimental set up.

considered, and a vapour separator is placed at the exit of the desorber. The leaving vapour stream is sent to the condenser (1) and the concentrated solution (8) is driven back to the absorber through the heat recoverer (9) and the throttling valve (10). The absorber is the component in the solution cycle that sucks the vapour at low pressure and low temperature (4) that condenses in the solution. The cooling water temperature determines the equilibrium exit condition of the solution (5), which is pumped (6) and preheated (7) before entering the desorber. The superheated vapour (1) condenses (2) at a rate and at a temperature that depend on both the vapour mass flow rate and the inlet temperature of the cooling water. The evaporation of the refrigerant (4) provides the cooling effect used to chill a given water flow rate (ch).

The LiBr H_2O chiller works by evaporating the refrigerant at temperatures ranging from 2 °C to 12 °C and providing a design cooling load of 7.5 kW. The plate heat exchangers considered in the study are commercially available PHEs. The plate surfaces are grooved with a corrugated sinusoidal shape and 60 ° chevron angle. The plate separation has been taken equal to 3 mm. The desorber, a 10-plate, 10 kW, one pass, counter current flow heat exchanger, is designed to provide a vapour stream of 11 kg/h. This mass flow rate of refrigerant condenses at a design temperature of 40 °C in an 8 kW condenser. The condenser is also configured as a one pass, counter current flow heat exchanger. Typically in PHEs, according to Ref. [17], the fouling factors are in the order of 0.1 m^2 K/kW. This is the value selected for the present calculation.

An experimental device with these specifications is being constructed and partially operated, including the desorber, the vapour separator and the condenser, as shown in Fig. 2.

3. Heat transfer and cycle simulation

As previously stated, in the present study, the properties of the working fluids are determined simultaneously with solving the thermodynamic cycle and the heat transfer equations in the plate heat exchangers.

In single phase, liquid to liquid plate heat exchangers, according to Ref. [4], there is still a lack of generalised thermal hydraulic predictive tools. Nevertheless, a general correlation for the Nusselt number of the kind,

$$Nu = C_1 Re^a Pr^{1/3} \tag{1}$$

is employed. The values of C_1 and a depend on the geometry of the plates [8]. For chevron plates at 60°, C_1 0.2 and a 0.7 as in Refs. [9,10]. These are the selected values to evaluate all the single phase heat transfer coefficients (both sides of the heat recoverer and external fluids in both the desorber and the condenser).

Some experimental works on condensation and evaporation in plate heat exchangers are available in the literature [7 10].

In the condenser, the Nusselt number for condensation is calculated using the correlation suggested in Ref. [8]:

$$Nu = C_2 Re_{eq}^b Pr^{1/3} \tag{2}$$

where Re_{eq} is the equivalent Reynolds number defined as

$$Re_{eq} = \frac{G_{eq} D_h}{\mu} \tag{3}$$

Here, G_{eq} is an equivalent mass flux as defined in Refs. [8 10]. The coefficients are C_2 3.2 and b 0.4 as in Ref. [8].

As far as we know, there are no available correlations to predict the boiling heat transfer coefficient for the LiBr H_2O solution in PHEs. Thus, an extension of some experimental works on evaporation is proposed. The correlation presented in Ref. [10] is used here:

$$Nu = C_3 Re^{0.7} Pr^{1/3} (C_4 Bo^{0.5}) \tag{4}$$

where Bo is the boiling number and C_3 0.2 and C_4 88. These are the constants used in the calculation of the Nusselt number in the desorber.

A further sensitivity analysis of the influence of the coefficients in each correlation is beyond the scope of the present work.

The thermodynamic properties of the solution and the refrigerant circulating through the chiller have been determined by the described cycles of the LiBr H_2O solution, and the refrigerant on the Dühring, Merkel and Mollier diagrams as in Ref. [3].

The inlet temperatures of the external fluids (cooling water in the absorber and the condenser and hot fluid in the desorber) are inputs, as well as the mass flow rates of the external fluids and the solution pumped. The vapour mass flow rate and the outlet temperatures are calculated by solving the heat transfer equations in both the desorber and the condenser. The absorption temperature was considered equal to the condensing temperature.

The iterative procedure begins in the desorber. The inlet temperature of the heating stream and its mass flow rate, as well as the solution mass flow rate, are known. The temperatures of the entering solution, the hot fluid and the solution outlet, as well as the separated refrigerant vapour mass flow rate, are initially guessed and used in the energy balance:

$$Q_{DES} = m_{Hf}(h_{Hfi} - h_{Hfo}) = (m_d - m_R)h_8 + m_R h_1 - m_d h_7 \tag{5}$$

Simultaneously, the heat transfer equation must be satisfied:

$$Q_{DES} = A_{DES} U_{DES} \Delta t_{DES} \tag{6}$$

where

$$U_{DES} = \frac{1}{\frac{1}{\alpha_{DES}} + R_{DES} + \frac{1}{\alpha_{Hf}}} \tag{7}$$

and

$$\Delta t_{DES} = \frac{(t_{Hfi} - t_8) - (t_{Hfo} - t_7)}{\ln\left(\frac{t_{Hfi} - t_8}{t_{Hfo} - t_7}\right)} \tag{8}$$

The heat transfer coefficients α_{DES} (solution side) and α_{Hf} (hot fluid side) are calculated with Eqs. (4) and (1), respectively. The wall conduction resistance is neglected for simplicity. The temperature of the entering solution to the desorber must also satisfy the conditions given in the heat recoverer, i.e. the heat transfer and energy equations:

$$Q_{RH} = A_{RH} U_{RH} \Delta t_{RH} \tag{9}$$

where

$$U_{RH} = \frac{1}{\frac{1}{\alpha_{RHh}} + R_{RH} + \frac{1}{\alpha_{RHc}}} \tag{10}$$

and

$$\Delta t_{RH} = \frac{(t_8 - t_7) - (t_{10} - t_5)}{\ln\left(\frac{t_8 - t_7}{t_{10} - t_5}\right)} \tag{11}$$

$$0 = m_d(h_7 - h_6) - (m_d - m_R)(h_8 - h_9) \tag{12}$$

The heat transfer coefficients α_{RHh} (hot side) and α_{RHc} (cold side) are calculated with Eq. (1).

The pump transports the diluted solution (rich in refrigerant) in the liquid state from the suction side (absorber) to the discharge side (desorber), increasing its pressure. We calculate the energy transferred by the pump w_P to the solution from the following energy balance,

$$w_P = m_d(h_6 - h_5) = m_d \cdot \frac{(P_{COND} - P_{ABS})}{\rho_d \cdot \eta_P} \tag{13}$$

The equilibrium temperature (and the corresponding pressure) in the absorber is obtained by transferring the absorption heat to the cooling water. By means of a mass and an energy balance in the absorber of Fig. 1, we obtain,

$$Q_{ABS} = m_{CWABS}(h_{CWABSo} - h_{CWABSi}) = m_R h_4 + (m_d - m_R)h_{10} - m_d h_5 \tag{14}$$

In the condenser, the energy and heat transfer equations must be satisfied:

$$Q_{COND} = m_{CWCOND}(h_{CWCONDo} - h_{CWCONDi}) = m_R(h_1 - h_2) \tag{15}$$

and

$$Q_{COND} = A_{COND} U_{COND} \Delta t_{COND} \tag{16}$$

where

$$U_{COND} = \frac{1}{\frac{1}{\alpha_{COND}} + R_{COND} + \frac{1}{\alpha_{CW}}} \tag{17}$$

and

$$\Delta t_{COND} = \frac{(t_1 - t_{CWo}) - (t_2 - t_{CWi})}{\ln\left(\frac{t_1 - t_{CWo}}{t_2 - t_{CWi}}\right)} \tag{18}$$

The heat transfer coefficients α_{COND} (vapour side) and α_{CW} (cooling water side) are calculated with Eqs. (2) and (1), respectively.

Finally, the evaporator heat transfer, i.e. the cooling load provided by the cycle, is calculated as

$$Q_E = m_{ch}(h_{chi} - h_{cho}) = m_R(h_4 - h_3) \tag{19}$$

Some preliminary experimental tests have already been performed in the PHEs that will be used as desorber and condenser in the prototype under construction. In order to investigate the validity of the heat transfer correlations selected from the literature, the desorber and the condenser have been experimentally and simultaneously tested with water as the evaporated and condensed fluid. The experimental set up is schematically shown in Fig. 2.

Water flows in the closed circuit. The experiment was heated by thermal oil at high temperature. The desorber (evaporator in these experiments) and the condenser are two Alfa Laval PHEs. All the generated vapour is sent to the condenser and condenses completely (this is assured by visual inspection through the sight glasses). To reduce the heat loss to the ambient, the heat exchangers were wrapped with 10 cm thick insulation. All the temperatures were measured by type T copper constantan thermocouples with a calibrated accuracy of ±1 °C. The thermal oil flow rate was measured with a rotameter (Rota Yokogawa) with an uncertainty of 3%. The cooling water flow rate was measured by a magnetic flow meter (Admeg SE Yokogawa) with an accuracy of 2%. An ultrasonic flow meter (Flexim) installed between the pump and the desorber measured the water pumped to the desorber. The accuracy in the measured water flow rate is ±5%. The experimental conditions are listed in Table 1.

On the one hand, the experimental heat supplied to the desorber Q_{DES} and the heat rejected in the condenser Q_{CON} are calculated using the measured properties of the external fluids and Eqs. (5) and (15), respectively. In steady state operation, both quantities should agree. The comparison of the heat balances, as shown in Fig. 3, succeeds fairly well within the range of the overall uncertainty in the measured heat rates, which is ±18%.

Table 1
Set of experimental parameters

Parameters	Measurements						
Heating fluid mass rate (kg/h)	3664	3669	3667	3869	2881	3640	3620
Water cooling mass rate (kg/h)	1110	1502	1505	218	595	2290	2090
Water pumped to the desorber (kg/h)	244	221	193	212	182	284	155
Cooling water temperature (°C)	20.4	24.1	26	21.8	19	19.1	21.2
Heating fluid temperature (°C)	112	103	107	102	114	105	114

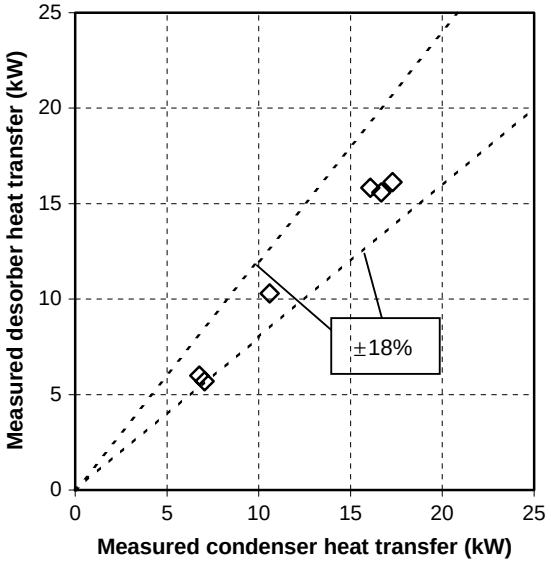

Fig. 3. Desorber and condenser measured heat transfer rates.

On the other hand, using the measured mass flow rates and the temperatures of the external streams, t_{Hfi} and t_{CWi}, the heat transfer coefficients are calculated with Eqs. (1) (4). The heat transfer problem is solved, and the resultant heat transfer rates in the desorber, Eqs. (6) (8) and the condenser, Eqs. (16) (18), are compared to the measured values (Fig. 4). The results compare well. The condenser presents a higher dispersion due to the uncertainty in the vapour mass flow rate, which is not directly measured.

The main interest in the present paper is to predict the performance of the absorption chiller operating with PHEs. These first results indicate that the heat transfer correlations selected seem correct for our purpose.

4. Results

The set of conditions for which Eqs. (1) (21) have been solved are the following: evaporation temperature ranging from 2 °C to 12 °C; inlet cooling water temperature ranging from 20 °C to 40 °C; heating fluid inlet temperature going from 75 °C to 115 °C (the lower value is limited by the condensing temperature, while the upper limit is imposed by the risk of crystallization). The first results correspond to a flow rate of 144 kg/h of solution pumped from the absorber. All the external flow rates are kept constant, equal to the design operating conditions (Table 2).

4.1. Performance at constant solution flow rate

The cooling effect and the coefficient of performance for a given evaporation temperature and desorber inlet temperature are shown in Figs. 5 and 6, respectively. In both figures, the expected behaviour is confirmed: the

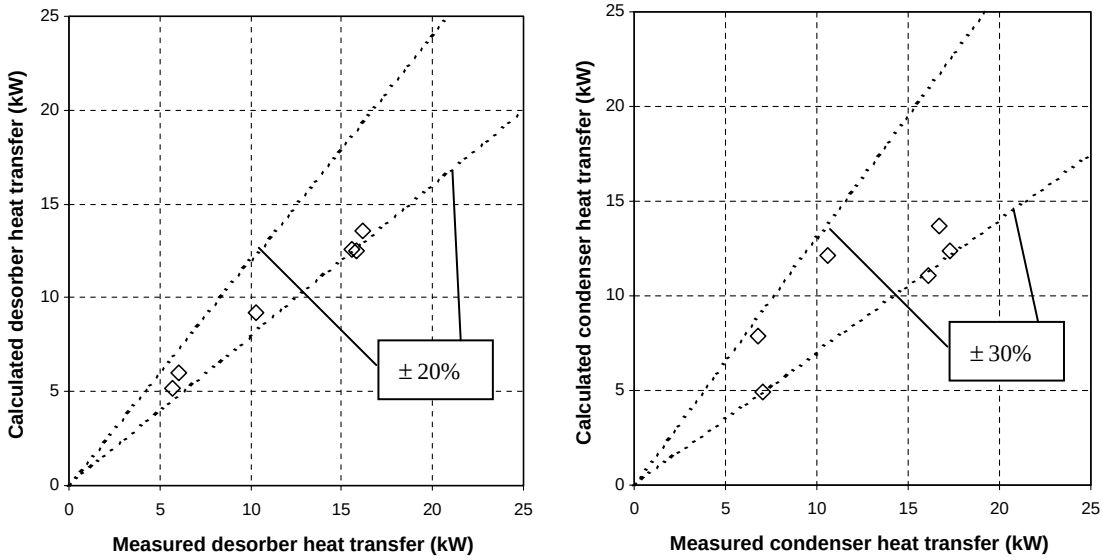

Fig. 4. Comparison of the measured and calculated heat transfer rates in the desorber (left) and the condenser (right).

Table 2
Design operation conditions

Design parameters	Results
Heating fluid mass rate: 1800 kg/h	$m_R = 11$ kg/h; $t_5 = 40$ °C
Water cooling mass rate: 1100 kg/h	$x_5 = 58\%$; $Q_E = 7.2$ kW
Solution pumped: 144 kg/h	$x_8 = 63\%$; $Q_{DES} = 10$ kW
Evaporating temperature: 5 °C	$t_8 = 90$ °C; $Q_{ABS} = 9.6$ kW
Cooling water temperature: 30 °C	$t_7 = 71$ °C; $Q_{COND} = 7.7$ kW
Heating fluid temperature: 100 °C	$t_{10} = 57$ °C; COP = 0.72

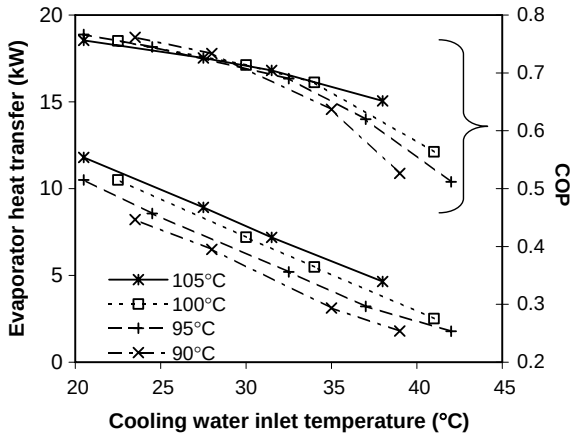

Fig. 5. Evaporator heat transfer (kW) and coefficient of performance (COP) for heating fluid temperature: 90 °C; 95 °C; 100 °C; 105 °C vs cooling water inlet temperature (°C). Evaporating temperature: 5 °C.

chilling capacity and the COP increase with the temperature of the heating fluid and the evaporation temperature, and they decrease with the cooling water temperature. The inlet temperature of the heating fluid does

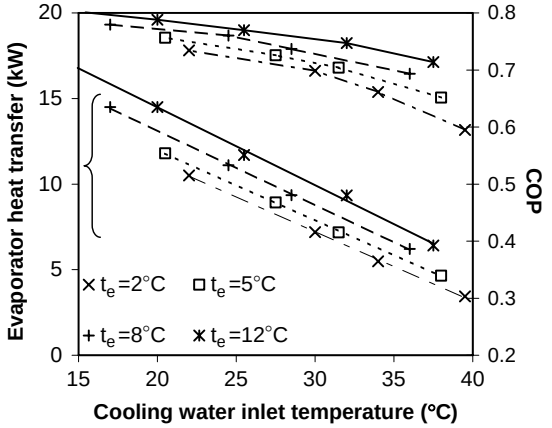

Fig. 6. Evaporator heat transfer (kW) and coefficient of performance (COP) for evaporation temperature: 2 °C; 5 °C; 8 °C; 12 °C vs cooling water inlet temperature (°C). Desorber inlet temperature: 105 °C.

not present a great influence on the COP (Fig. 5). In comparison, the evaporation temperature greatly affects the COP (Fig. 6).

A better understanding of the operation of the chiller may be seen in Fig. 7. The internal parameters of the absorption cycle, such as the condensing temperature and the concentration of the solution are represented as a function of the inlet temperature of the heating fluid and the cooling water inlet temperature. The calculated chilling load is also represented. The evaporating temperature is kept constant at 5 °C. This is, for example, a condition to have chilled water at around 13 °C for an air conditioning system.

As an example, for a given cooling load of 7 kW, the chiller may be operated with a heating source at 85 °C when the water cooling temperature is 26 °C. These conditions result in a condenser temperature of 35 °C. It

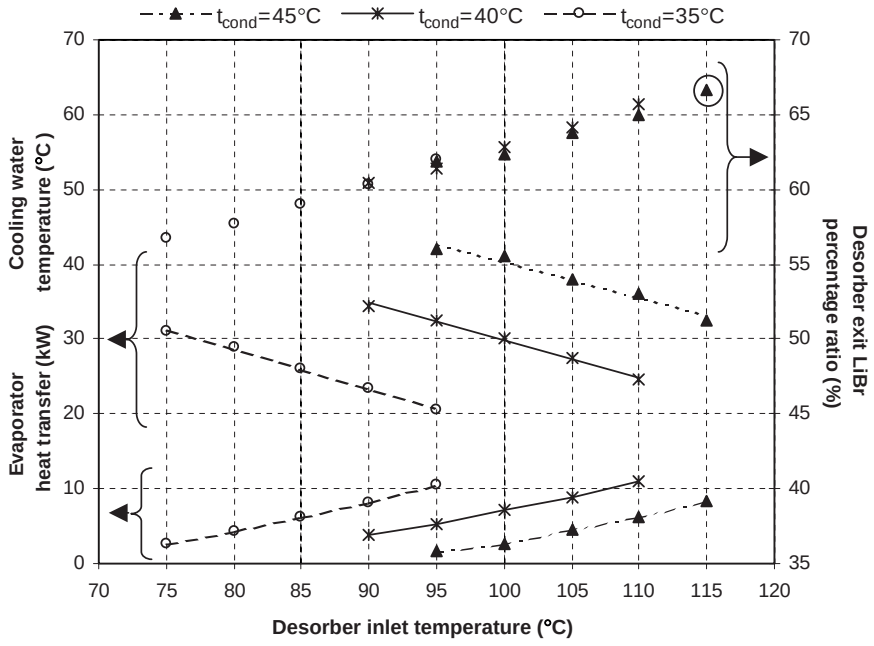

Fig. 7. Cooling load (kW), condensing temperature ($t_{cond} = 35$ °C; 40 °C and 45 °C) and desorber exit LiBr percentage ratio (%) vs desorber inlet temperature (°C) and cooling water temperature (°C). Evaporating temperature: 5 °C.

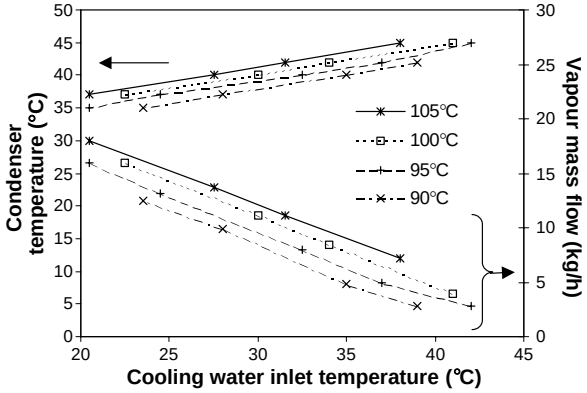

Fig. 8. Vapour mass flow (kg/h) and condenser temperature (°C) vs cooling water inlet temperature (°C) for heating fluid temperatures: 90 °C; 95 °C; 100 °C; 105 °C. Evaporator temperature: 5 °C.

will also be possible to obtain the same refrigerating capacity by heating the desorber at 97 °C at a higher outside temperature (32 °C). In this last case, the condenser temperature will also be higher (40 °C).

In the present case, the correlation used for the plate heat exchanger in the condenser side establishes the relationship between the saturation temperature and the cooling water temperature. Fig. 8 shows how the increase in the temperature of the heating source is followed by an increase in the generated refrigerant vapour. This leads to an increase in the condenser pressure as a result of the higher quantity of refrigerant vapour in the condenser. Consequently, the condenser temperature increases.

In real operation, the outside temperature may increase. This increase will be followed by an increase in the cooling duty. The condensation temperature can only be kept constant by an increase in the temperature of

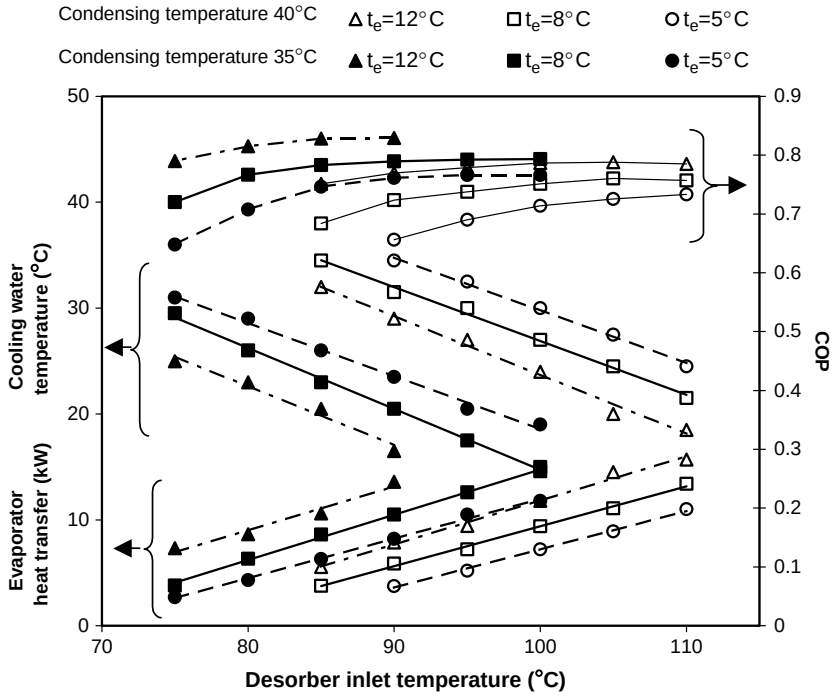

Fig. 9. Evaporator heat transfer (kW) and COP vs desorber inlet temperature (°C) and cooling water temperature (°C). Condensation temperatures: 35 °C and 40 °C; Evaporation temperatures: 5 °C; 8 °C and 12 °C.

the heating source (see Fig. 7). For example, for a given load of 8 kW with an outside temperature of 30 °C, while the desorber is fed at 100 °C, the condenser temperature is 40 °C. If the outside temperature reaches 40 °C, without modifying the temperature of the heating source, the refrigeration capacity will fall to 3 kW (and the condensing temperature will be above 45 °C). As a consequence, to maintain the load, the heating source has to be at a higher temperature (at least 112 °C), to provide a load of 8 kW. In such a case, the condenser temperature will be equal to 45 °C, and the limit of crystallization will be closer, as it is shown by the exit solution concentration (65%) in Fig. 7. In this figure, the encircled operated condition (condensing at 45 °C and heating the desorber at 115 °C) results in a too high concentration at the desorber outlet.

The above example illustrates one way to control the operation of the chiller in an off design condition, varying the desorber inlet heating temperature.

All the external operating conditions and the resultant performance values (cooling load and COP) are shown in Fig. 9. The temperatures of the external fluids determine the condensing temperatures for all the

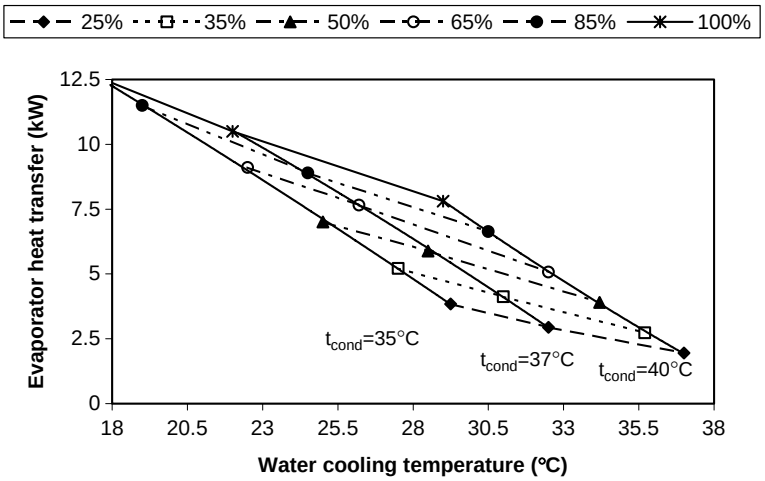

Fig. 10. Evaporator heat transfer (kW) vs water cooling temperature (°C) at different solution flow rates, as a % of design load. Heating in the desorber: 100 °C. Evaporating temperature: 5 °C.

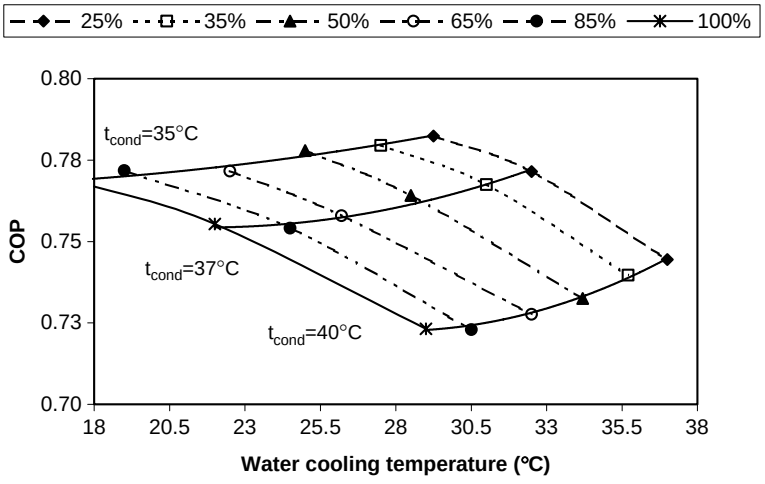

Fig. 11. COP vs water cooling temperature (°C) at different solution flow rates, as a % of design load. Heating in the desorber: 100 °C. Evaporating temperature: 5 °C.

possible evaporating conditions. In this way, for the present absorption chiller, it is possible to predict its complete performance.

4.2. Part load operation: solution flow rate control

One of the methods to reduce the refrigerating capacity of the absorption unit is to reduce the solution flow delivered by the pump. A reduction in the generated vapour mass flow rate and, consequently, a decrease in the cooling effect (Fig. 10) follow this reduction. Simultaneously, the condensing temperature decreases, as less vapour enters the condenser, and therefore, a decrease in the condenser pressure follows.

According to Fig. 11, at part load, for a given mass flow rate of solution pumped, the COP increases as the outside temperature decreases. This decrease is followed by a decrease in the condensing temperature.

For a given cooling water temperature, as the solution circulation decreases, the COP increases due to the decrease in the condensing temperature and also due to the fact that the solution to refrigerant ratio decreases, as shown in Fig. 12.

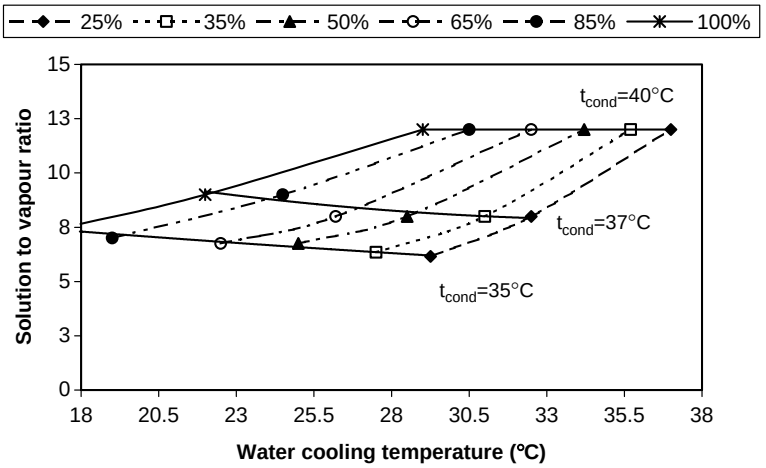

Fig. 12. Solution to vapour mass flow ratio vs water cooling temperature (°C) at different solution flow rates, as a % of design load. Heating in the desorber: 100 °C. Evaporating temperature: 5 °C.

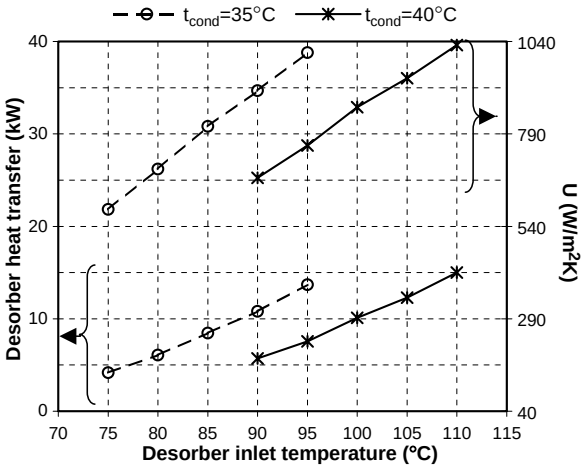

Fig. 13. Desorber heat transfer (kW) and global heat coefficient (U, W/m^2 K) vs desorber inlet temperature (°C). Condenser temperatures: 35 °C; 40 °C. Evaporating temperature: 5 °C.

4.3. Heat transfer

The analysis of the desorber plate heat exchanger is shown in Fig. 13. As the heating temperature increases, a higher wall superheat occurs. This gives a higher water vapour production (see the desorber outlet concentration in Fig. 7). In accordance with Refs. [7,10] the boiling heat transfer coefficient increases as a result of a higher nucleation density on the plate and, therefore, a higher bubble generation frequency. The rise in the heat transfer is more pronounced as not only the heat transfer coefficient is higher but also the driving temperature.

The condenser performance is represented in Fig. 14. For a given water cooling inlet temperature, the heat rejected increases for higher condensing temperatures at an approximate rate of 0.73 kW/K. A higher heating temperature is also needed. The behaviour of the condenser can be represented by the following relationship:

$$Q_{\mathrm{COND}} = 0.73(t_{\mathrm{COND}} - t_{\mathrm{CWi}}) \tag{20}$$

The performance of the heat recoverer is shown in Fig. 15 as a function of the hot solution inlet temperature in the heat recoverer (t_8 in Fig. 1). The heat recoverer efficiency is calculated as the ratio between the

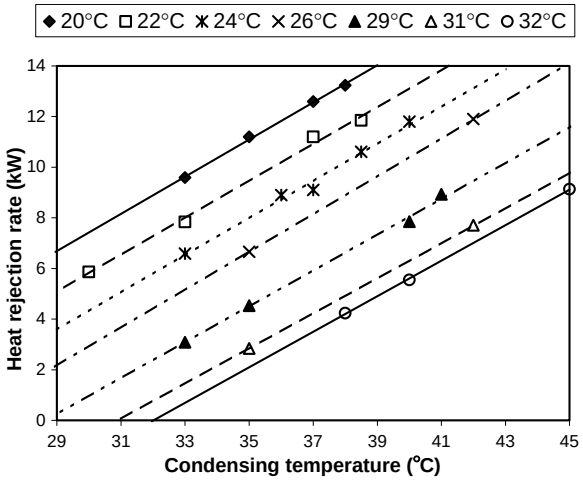

Fig. 14. Performance of the PHE condenser (kW) vs condensing temperature (°C) at different water cooling inlet temperatures.

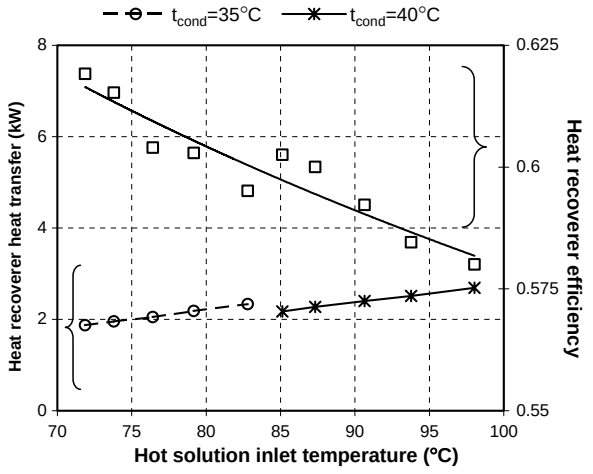

Fig. 15. Heat recoverer performance (kW) and efficiency vs hot solution inlet temperature into the heat recoverer at 35 °C and 40 °C condensing temperatures.

heat exchanged between the rich and the poor solution to the maximum heat that both currents could exchange:

$$\mathrm{Eff} = \frac{Q_{\mathrm{RH}}}{Q_{\mathrm{MAX}}} = \frac{(m_{\mathrm{d}} - m_{\mathrm{R}})c_{\mathrm{Pd}}(t_8 - t_{10})}{(m_{\mathrm{d}} - m_{\mathrm{R}})c_{\mathrm{Pd}}(t_8 - t_6)} \tag{21}$$

The heat recoverer loses efficiency when working at higher temperature levels at a rate of 0.1%/K.

5. Conclusions

A LiBr water absorption system configured with plate heat exchangers in the desorber, the condenser and the heat recoverer is considered. This system has the advantage of a higher chilling capacity to volume ratio.

The thermodynamic cycle has been solved simultaneously with the heat transfer equations of the selected plate heat exchangers. The heat transfer correlations employed, taken from the literature, have already been experimentally validated in the desorber and the condenser with water as the evaporated and condensed fluid.

In this way, the operating conditions are defined according to the more realistic driving temperatures, i.e. the temperatures of the external fluids. Therefore, an arbitrary selection of the condensing and final desorption temperatures is avoided. The design and part load characteristics have been investigated for a complete set of external temperatures. The result can be used as a performance predictive tool.

High COPs, as high as 0.8, have been found, but only for low ambient temperatures (around 20 °C). At higher ambient temperatures (more than 30 °C), the COP approximates 0.75 but at the expense of higher heating temperatures.

Off design operation has been analysed in two ways: controlling the heating source and controlling the circulated solution flow rate. In the first case, special care has to be taken to avoid crystallization. In the second case, at part load, when the circulating solution decreases, the decrease in the vapour flux is more pronounced, and the solution to refrigerant ratio decreases. As a consequence, the COP increases.

Acknowledgement

This work was partially funded by CICYT Ministerio de Ciencia y Tecnología (CLIMABCAR project no. DPI 2003-01567).

References

[1] Lamp P, Ziegler F. European research on solar assisted air conditioning. Int J Refrig 1998;21(2):89–99.
[2] Filipe Mendes L, Collares Pereira M, Ziegler F. Supply of cooling and heating with solar assisted absorption heat pumps: an energetic approach. Int J Refrig 1998;21(2):116–25.
[3] Izquierdo M, de Vega M, Lecuona A, Rodríguez P. Compressors driven by thermal solar energy: entropy generated, exergy destroyed and exergetic efficiency. Sol Energy 2002;72(4):363–75.
[4] Manglik RM. Plate heat exchangers for process industry applications: enhanced thermal–hydraulic characteristics of chevron plates. In: Manglik RM, Kraus AD, editors. Process enhanced and multiphase heat transfer. Begell House; 1996. p. 267–76.
[5] Muley A, Manglik RM. Experimental study of turbulent flow heat transfer and pressure drop in a plate heat exchanger with chevron plates. Trans ASME 1999;121:110–7.
[6] Martin H. A theoretical approach to predict the performance of chevron type plate heat exchangers. Chem Eng Process 1996;35:301–10.
[7] Watel B. Review of saturated flow boiling in small passages of compact heat exchangers. Int J Therm Sci 2003;42:107–40.
[8] Wurfel R, Ostrowski N. Experimental investigations of heat transfer and pressure drop during the condensation process within plate heat exchangers of the herringbone type. Int J Therm Sci 2004;43:59–68.
[9] Yan Y Y, Lio H C, Lin T F. Condensation heat transfer and pressure drop of refrigerant R-134a in a plate heat exchanger. Int J Heat Mass Trans 1999;42:993–1006.
[10] Hsieh YY, Lin TF. Saturated flow boiling heat transfer and pressure drop of refrigerant R-410A in a vertical plate heat exchanger. Int J Heat Mass Trans 2002;45:1033–44.
[11] Flamensbeck M, Summerer F, Riesch P, Ziegler F, Alefeld G. A cost effective absorption chiller with plate heat exchangers using water and hydroxides. Appl Therm Eng 1998;18(6):413–25.
[12] Vallès M, Bourouis M, Boer D, Coronas A. Absorption of organic fluid mixtures in plate heat exchangers. Int J Therm Sci 2003;42:85–94.

[13] Herold KE, Radermacher R, Klein SA. Absorption chillers and heat pumps. CRC Press, Inc; 1996.
[14] Romero RJ, Rivera W, Gracia J, Best R. Theoretical comparison of performance of an absorption heat pump system for cooling and heating operating with an aqueous ternary hydroxide and water/lithium bromide. Appl Therm Eng 2001;21:1137 47.
[15] Saravanan R, Maiya MP. Effect of component pressure drops in two fluid pumpless continuous vapour absorption refrigerator. Energ Convers Manage 1997;38(18):1823 32.
[16] Florides GA, Kalogirou SA, Tassou SA, Wrobel LC. Design and construction of a LiBr water absorption machine. Energ Convers Manage 2003;44:2483 508.
[17] Hesselgreaves JE. An approach to fouling allowances in the design of compact heat exchangers. Appl Therm Eng 2002;22:755 62.